Available online at www.sciencedirect.com
SCIENCE DIRECT
Diamond & Related Materials 15 (2006) 212 – 216
DIAMOND AND RELATED MATERIALS
www.elsevier.com/locate/diamond

Stability of field emission current from various types of carbon nanotube films

Benjamin Ulmen, Vijaya Kumar Kayastha, Adam DeConinck, Jiesheng Wang, Yoke Khin Yap *

Department of Physics, Michigan Technological University, 118 Fisher Hall, 1400 Townsend Dr., Houghton, MI 49931, USA

Available online 19 September 2005

Abstract

A series of emission current measurements were taken from various types of multiwalled carbon nanotube (MWCNT) films in order to examine their stability for electron field emission. We found that the MWCNTs films grown by the catalytic thermal chemical vapor deposition (CVD) method exhibited much improved emission stability as compared to MWCNT films grown by the plasma-enhanced CVD (PECVD) method. We explain this difference of performance by referring to the graphitic order of these MWCNTs as detected by transmission electron microscopy and Raman spectroscopy. Results indicate that MWCNTs with high-order tubular structures demonstrate stable electron field emission. The best performing sample exhibits a constant current degradation of ~3% per hour at an emission current density of ~1 mJ/cm^2.

Keywords: Display technologies; Field emission; Nanotubes; Defects

1. Introduction

Carbon nanotubes (CNTs) are well known for their exceptional field emission properties [1,2]. The multitude of applications for CNT field emitters, including electron microscopy [3], display devices [4,5], vacuum electronics [6], luminescent tubes [7], gas discharge tubes [8], and X-ray tubes [9], have caused this to become an exciting and promising area of research. Before this novel material can be made ready for commercial use, stability of the devices must be considered [10,11]. We have studied the degradation of the emission current from multiwalled carbon nanotubes (MWCNTs) grown over a range of conditions and by the techniques of plasma-enhanced chemical vapor deposition (PECVD) and catalytic thermal chemical vapor deposition.

Our PECVD system is a dual-RF plasma system [12,13]. The nanotubes created by this system have potential for field emission because of the natural vertical alignment caused by the electric field. According to FESEM, these nanotubes tend to be shorter (a few microns) and thick in diameter (~50–200 nm). The structural order of these MWCNTs is inferior to those grown by arc discharge. Sometimes, they are referred to as carbon nanofibers. On the other hand, random and aligned MWCNTs can be grown by our catalytic thermal CVD with and without the use of ammonia gas [14]. These nanotubes have a higher field enhancement factor caused by their slender diameter (~5 to 10 nm) and significant length (~tens of micrometers). These MWCNTs have higher graphitic order that those grown by PECVD as indicated by both transmission electron microscopy and Raman spectroscopy [14,15]. We found that the catalytic thermal CVD system can produce nanotubes capable of excellent emission currents at lower voltages.

2. Experiments

The system we have used to make our electron field emission measurements contains several features to optimize the accuracy of the measurements. We have created a "hanging" electrode design to maintain a precise spacing without the use of dielectric spacers in close proximity to the sample as shown in Fig. 1. This minimizes dielectric current leak. The distance between the bottom electrode (cathode) and the hanging top electrode (anode) was precisely adjusted to 1000±10 μm. The MWCNTs films were all coated on low resistivity (1 Ω cm^{-1}) Si substrates. The substrates were placed on top of the bottom electrodes and held by silver paste. The substrate thickness of all MWCNTs films was measured precisely by a mechanical micrometer, typically ~425 μm. By knowing the substrate

* Corresponding author. Tel.: +1 906 487 2900; fax: +1 906 487 2933.
E-mail address: ykyap@mtu.edu (Y.K. Yap).

0925-9635/$ - see front matter © 2005 Elsevier B.V. All rights reserved.
doi:10.1016/j.diamond.2005.08.040

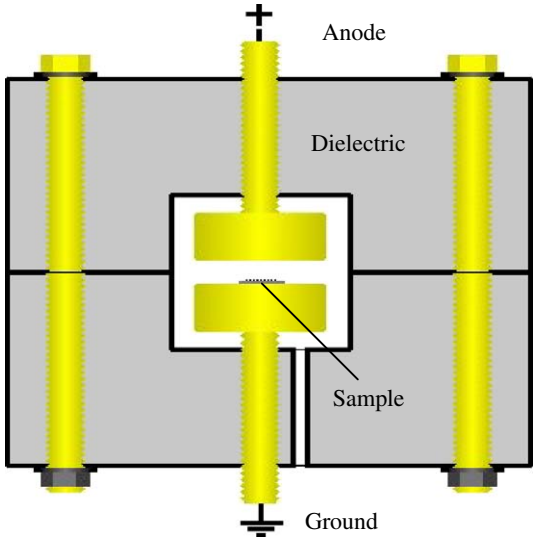

Fig. 1. Setup for the measurement of electron field emission.

thickness, the actual distance between the growth surface and the top electrode can be calculated. Then these measurement stages were installed inside a stainless steel high-vacuum chamber. The chamber was always evacuated to $\sim 2.0 \times 10^{-7}$ mbar before the experiments and maintained during the field emission measurements.

3. Results and discussions

3.1. Field emission from PECVD grown MWCNTs

According to the Fowler–Nordheim (F–N) equation, electron field emission from nanotubes depends on the aspect ratios (tubular length to tubular radius) and spacing between the MWCNTs. Thus we have characterized three types of MWCNTs films grown by PECVD: short and thick MWCNTs, long and thin MWCNTs, and long, thin, and sparse MWCNTs. The growth mode of these MWCNTs was controlled by the thickness of the Ni catalyst films and the plasma configurations as described elsewhere [13].

3.1.1. Field emission from short and thick MWCNTs

We have tested a sample with diameters of ~70–200 nm and ~1.5 μm long as shown in Fig. 2(a). We found that stable emission current density measurement (J–E) cannot be obtained even at high vacuum condition. We then conducted a conditioning process on the sample by extended duration application of an electric field across the sample producing an initial current density of ~300 μA/cm^2. As shown in Fig. 2(b), the emitted current dropped off rapidly in the first 200 min and gained stable emission after ~400 min at a level of ~50 μA/cm^2. As shown, some current spikes are still detected after conditioning for more than 400 min. After the conditioning, stable J–E curve can be obtained as shown in Fig. 2(c) with an emission threshold of ~4.3 V/μm. The threshold electric field, E_{th} is defined as the electric field needed for emitting electron at a level of 1 μA/cm^2. The corresponding F–N plot for this sample is shown in Fig. 2(d), which indicates that electrons are released to the vacuum by quantum tunneling [1,2].

3.1.2. Field emission from long and thin MWCNTs

Similar behaviors were detected from a sample that has longer and thinner MWCNTs. As shown in Fig. 3(a), these MWCNTs are as long as 3 μm and have nominal diameters of

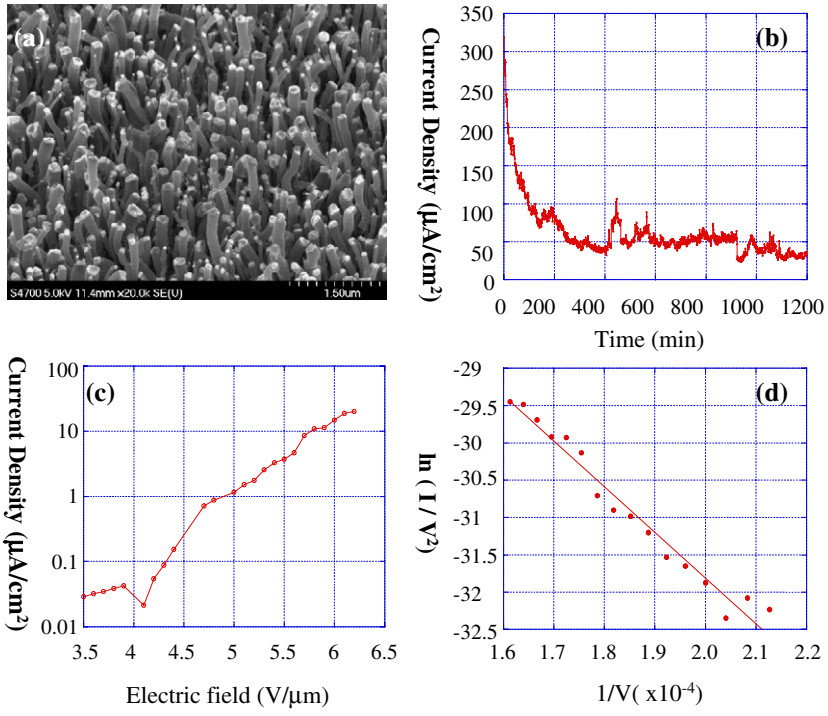

Fig. 2. (a) Images of the short and thick MWCNTs, their related (b) conditioning curve, (c) J–E curve, and (d) F–N plot.

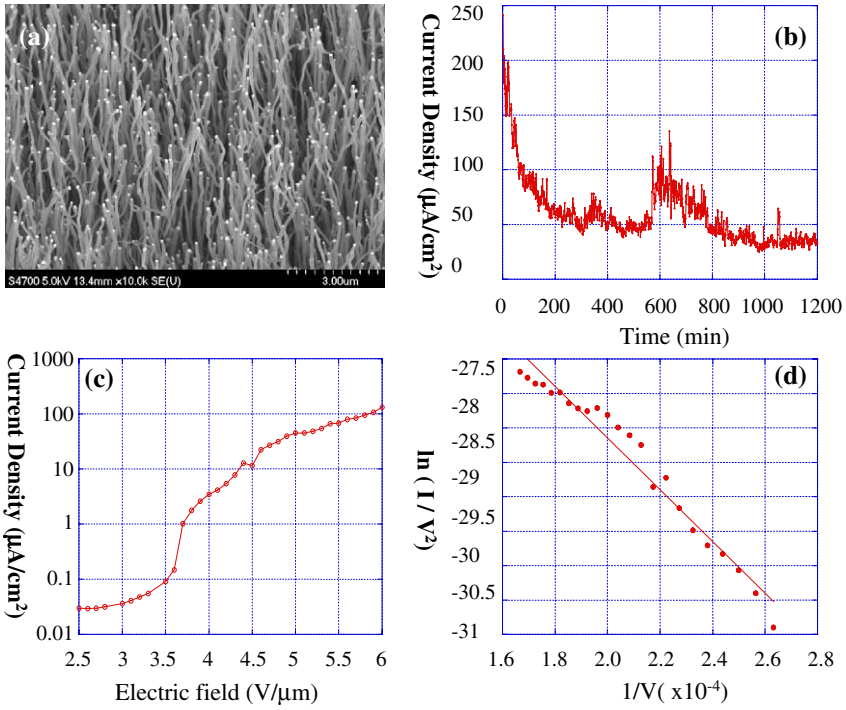

Fig. 3. (a) Images of the long and thin MWCNTs, their related (b) conditioning curve, (c) J–E curve, and (d) F–N plot.

~100 nm. Again, stable emission cannot be obtained without the conditioning process. As shown in Fig. 3(b), the emission becomes relatively stable after ~400 min at a level of ~50 μA/cm^2. The J–E curve in Fig. 3(c) indicates that E_{th} ~3.7 V/μm, probably due to the higher aspect ratio of the MWCNTs. Again, a straight F–N plot is obtained as shown in Fig. 3(d) and indicating an electron tunneling process from MWCNTs to the vacuum.

3.1.3. Field emission from long, thin, and sparse MWCNTs

We then tested a sample with sparse density as shown in Fig. 4(a). These MWCNTs are as long as 3 μm and having nominal diameters of ~50 nm at their tips. We are particularly interested on this sample since their morphologies are quite ideal for good electron field emission: long, sharp tips and sparse in distribution, which can have high electric field enhancement factor at their tips with re-

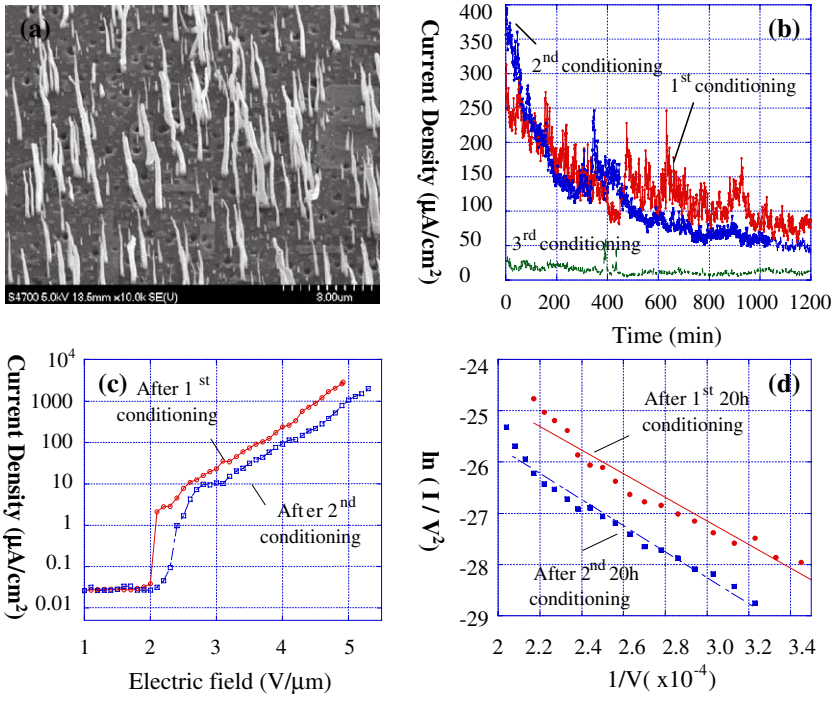

Fig. 4. (a) Images of the long, sharp, and sparse MWCNTs, their related (b) conditioning curves, (c) J–E curves, and (d) F–N plots.

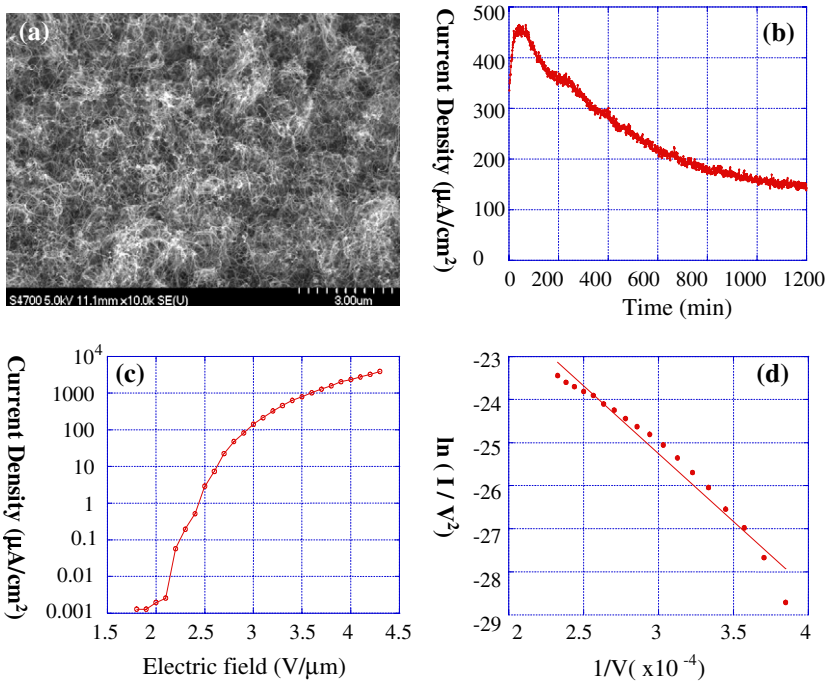

Fig. 5. (a) Images of the thermal CVD grown MWCNTs, their related (b) conditioning curve, (c) J–E curve, and (d) F–N plot.

duced electric field screening effects from adjacent MWCNTs [16].

As usual, we need to condition the sample. We observed that this sample is quite noisy in emission during the first conditioning process as shown in Fig. 4(b). A J–E curve can be obtained after the first conditioning as shown in Fig. 4(c). As expected, this sample has E_{th} ~2.1 V/μm, much lower that the previously tested samples. After the J–E measurement, we conducted the second conditioning process. To our surprise, the emission current dropped off rapidly from an initial current density of ~300 μA/cm^2, despite the fact that it has been conditioned once. However, we did observe a less noisy signal. After the second conditioning, we repeated the I–E measurement as shown in Fig. 4(c). We found that the I–E curve is quite reproducible with a E_{th} ~2.4 V/μm. We then tested the emission stability at a current density of ~30 μA/cm^2, approximately one tenth the initial value. This is shown as the 3rd conditioning in Fig. 4(b). As shown, the emitted current is stable for 1200 min although two current spikes are detected at ~400 min. In Fig. 4(d), F–N plots for the two tested J–E curve indicate that electron tunneling was responsible for the detected current.

3.2. Field emission from thermal CVD grown MWCNTs

We repeated the experiment on samples grown by thermal CVD by C_2H_2/Ar mixed gas and Fe catalyst [14,15]. As shown in Fig. 5(a), these samples have randomly grown MWCNTs. One of the representing conditioning behaviors of these samples is shown in Fig. 5(b). As shown, the emitting current increases from ~300 to ~450 μA/cm^2 in the first one hour. The emitted current starts to drop off to about one third of its peak value after 1200 min. This degradation is significantly smaller than those detected from PECVD grown samples. Furthermore, some thermal CVD grown samples did not indicate serious current degradation during the conditioning process after 1200 min. These samples usually indicate cleaner J–E curves as compared to the PECVD grown MWCNTs discussed earlier and with lower E_{th} (~1.7 V/μm) as shown in Fig. 5(c). As indicated by the F–N plot in Fig. 5(d), the collected data originated from electron tunneling.

We found that MWCNTs grown by thermal CVD has much better emission stability. One of the best data is shown in Fig. 6. As shown, the field emission current degraded at a constant rate of ~3% per hour. Since both the PECVD and thermal CVD grown samples are tested in the same system and high vacuum condition, the different performance discussed so far should be related to their intrinsic structural properties. Fig. 7 shows that MWCNTs grown by (a) thermal

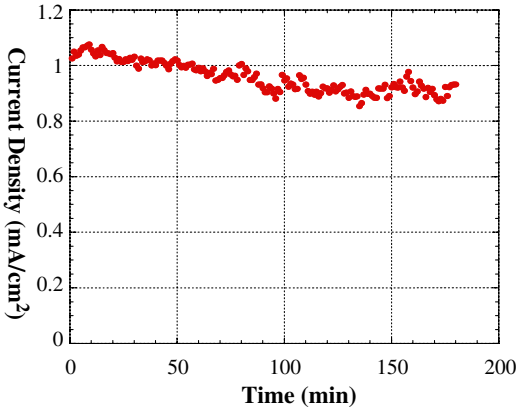

Fig. 6. Stability test of a thermal CVD grown sample.

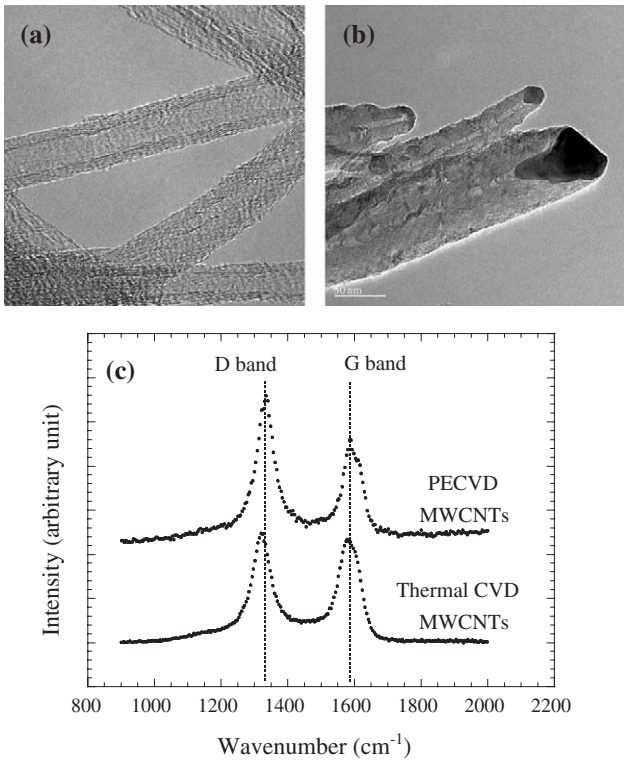

Fig. 7. Typical structures of MWCNTs grown by (a) thermal CVD and (b) PECVD. (c) Raman spectra for both types of MWCNTs are shown for comparison.

CVD are having higher structural order than MWCNTs grown by (b) PECVD. Raman spectroscopy also indicates a higher graphitic order in MWCNTs grown by thermal CVD. The relative intensity of the graphitic (G) band to the disorder (D) band is higher for MWCNTs grown by thermal CVD. We think that the high-order tubular structures of our thermal CVD grown MWCNTs is responsible for their stable field emission characters.

4. Conclusion

We have tested various types of MWCNTs grown by both PECVD and catalytic thermal CVD. All samples required a conditioning process for obtaining stable J–E measurement. We found that PECVD grown MWCNTs have poor stability when emitting at high current density (hundreds of $\mu A/cm^2$) but are very stable for 20 h when emitting at a level of several tens of $\mu A/cm^2$. On the other hand, MWCNTs grown by thermal CVD demonstrate low current degradation of 3% per hour at current density of 1 mA/cm^2. Higher stabilities are expected at lower current density and vice versa. The excellent emission stability of the thermal CVD grown MWCNTs are due to their high-order tubular structures.

Acknowledgement

Y. K. Y acknowledges supports from Michigan Tech Research Excellent Fund, the Department of Army (W911NF-04-1-0029, through the City College of New York), and the Center for Nanophase Materials Sciences (sponsored by the Division of Materials Sciences and Engineering, U.S. Department of Energy, under contract DE-AC05-00OR22725 with UT-Battelle, LLC).

References

[1] W.A. de Heer, A. Châtelain, D. Ugarte, Science 270 (1995) 1179.
[2] P.G. Collins, A. Zettl, Appl. Phys. Lett. 65 (1996) 1969.
[3] N. de Jonge, Y. Lamy, K. Schoots, T.H. Oosterkamp, Nature 420 (2002) 393.
[4] Q.H. Wang, A.A. Setlur, J.M. Lauerhaas, J.Y. Dai, E.W. Seelig, R.P.H. Chang, Appl. Phys. Lett. 72 (1998) 2912.
[5] W.B. Choi, D.S. Chung, J.H. Kang, H.Y. Kim, Y.W. Jin, I.T. Han, Y.H. Lee, J.E. Jung, N.S. Lee, G.S. Park, J.M. Kim, Appl. Phys. Lett. 75 (1999) 3129.
[6] D.S.Y. Hsu, J. Shaw, Appl. Phys. Lett. 80 (2002) 118.
[7] J.-M. Bonard, T. Stöckli, O. Noury, A. Cha telain, Appl. Phys. Lett. 78 (2001) 2775.
[8] R. Rosen, W. Simendinger, C. Debbault, H. Shimoda, L. Fleming, B. Stoner, O. Zhou, Appl. Phys. Lett. 76 (2000) 1668.
[9] G.Z. Yue, Q. Qiu, B. Gao, Y. Cheng, J. Zhang, H. Shimoda, S. Chang, J.P. Lu, O. Zhou, Appl. Phys. Lett. 81 (2002) 355.
[10] J.-M. Bonard, C. Klinke, K.A. Dean, B.F. Coll, Phys. Rev., B 67 (2003) 115406.
[11] Y. Wei, Chenggang Xie, Kenneth A. Dean, Bernard F. Coll, Appl. Phys. Lett. 79 (2001) 4527.
[12] T. Hirao, K. Ito, H. Furuta, Y.K. Yap, T. Ikuno, S. Honda, Y. Mori, T. Sasaki, K. Oura, Jpn. J. Appl. Phys. 40 (2001) L631.
[13] J. Menda, K.L. Vanga, B. Ulmen, Y.K. Yap, Z. Pan, I.N. Ivanov, A.A. Puretzky, D.B. Geohegan, Mater. Res. Soc. Symp. Proc. 858E (2005) (paper HH3.11).
[14] V. Kayastha, Y.K. Yap, S. Dimovski, Y. Gogotsi, Appl. Phys. Lett. 85 (2004) 3265.
[15] V. Kayastha, Y.K. Yap, Z. Pan, I.N. Ivanov, A.A. Puretzky, D.B. Geohegan, Appl. Phys. Lett. 86 (2005) 253105.
[16] L. Nilsson, O. Groening, C. Emmenegger, O. Kuettel, E. Schaller, L. Schlapbach, H. Kind, J.-M. Bonard, K. Kern, Appl. Phys. Lett. 76 (2000) 2071.